Microchimica Acta (2022) 189: 137
https://doi.org/10.1007/s00604-022-05249-x

ORIGINAL PAPER

Molecularly imprinted ratiometric electrochemical sensor based on carbon nanotubes/cuprous oxide nanoparticles/titanium carbide MXene composite for diethylstilbestrol detection

Yide Xia[1] · Xiaopeng Hu[1] · Yiwei Liu[1] · Faqiong Zhao[1] · Baizhao Zeng[1]

Received: 22 December 2021 / Accepted: 23 February 2022 / Published online: 9 March 2022

Abstract

Conventional molecularly imprinted polymers (MIP)–based electrochemical sensors are generally susceptible to the changes of personal operation, electrode surface, and solution conditions. Herein, a ratiometric strategy was employed through introducing Cu_2O nanoparticles (NPs) as inner reference probe to realize the reliable detection of diethylstilbestrol (DES). MIP film was prepared by electropolymerization of 1H-pyrrole-3-carboxylicacid in the presence of DES on carbon nanotubes/cuprous oxide/titanium carbide (CNT/Cu_2O NPs/$Ti_3C_2T_x$) modified electrodes. The $Ti_3C_2T_x$ with accordion-like structure not only possessed good electrical conductivity, but also facilitated the immobilization of Cu_2O NPs, which contributed to stabilizing the signal. CNT was introduced to further improve the sensitivity of the sensor. Under optimum conditions, the MIP/CNT/Cu_2O NPs/$Ti_3C_2T_x$ electrochemical sensors showed a broad linear response range of 0.01 to 70 μM, and a low detection limit of 6 nM ($S/N = 3$). Moreover, the sensor was applied to detect DES in real samples including lake water, milk, and pork, and the recoveries for spiked standard were 88–112%. Thus, this work provides a new way for reliable DES detection.

Keywords Electrochemical sensors · Molecularly imprinted polymers · Ratiometric strategy · Diethylstilbestrol · Titanium carbide · Cuprous oxide

Introduction

Diethylstilbestrol (DES) is a representative kind of synthetic exogenous estrogen which is often used as the animal growth promoter and widely applied in veterinary medicine to treat estrogen deficiency [1]. However, DES can be absorbed by human body through food chain and combined with estrogen receptor, competing with endogenous estradiol, resulting in the disorder of human hormones and endocrine system [2]. Compared with the natural estrogen, DES is more stable and can stay in the human body for a long time, relevant researches manifest that DES can cause cancer [3]. DES has been prohibited by China, the USA, Japan, and the European Union for all food animals [4]. Therefore, monitoring the content of DES existing in the environment and foods (e.g., milk, meat) is of great significance. Various detection techniques including high-performance liquid chromatography [5], gas chromatography coupled with mass spectrometry [6], capillary electrochromatography [7], enzyme-linked immunosorbent assay [8], and immunoassay [9] have been applied to detect DES. However, these methods are either time-consuming or expensive. Electrochemical method has aroused widespread concern of researches for its easy operation and fast detection [10, 11].

Numerous researches have reported on the electrochemical detection of DES [12, 13]. For example, Yang et al. determined DES using a CeO_2 nanorod/graphene nanoplatelet-modified electrode, with a low limit of detection of 1.5 nM [12]. In another report, DES was determined based on its electrochemical oxidation on a Cu-MOF–modified carbon paste electrode, the limit of detection was 2.7 nM [13]. However, such electrochemical sensors typically distinguish interferences by oxidation potential, so the selectivity is easily affected when the oxidation potential of interferences are close to DES. Therefore, to further

✉ Baizhao Zeng
bzzeng@whu.edu.cn

[1] College of Chemistry and Molecular Sciences, Wuhan University, Wuhan 430072, Hubei Province, People's Republic of China

improve the selectivity of electrochemical senor of DES is significant.

Molecularly imprinted polymers (MIP), as the biomimic material for selective recognition, have been widely applied to improve the selectivity of electrochemical sensors [14]. However, the response of MIP electrochemical sensor toward target is easily disturbed by the unavoidable factors, including the variations in the fabrication process of electrodes and the pollution of electrode surface [15, 16]. Fortunately, the ratiometric sensing strategy can effectively reduce the fluctuation of output signal [17], as the inner reference signal can correct the influence of various factors by using the ratio of the detection signal and inner reference signal as output signal. Therefore, ratiometric MIP electrochemical sensor can provide more reliable data with satisfactory selectivity. But so far, only a few researches on ratiometric molecularly imprinted electrochemical sensor have been reported [16, 18].

However, the immobilization process of inner reference substances (e.g., ferrocene and thionine) on electrode surface is complex, and usually involves electropolymerization or covalent coupling, which limited the application of ratiometric electrochemical sensor [19]. For this reason, it is of great significance to choose an appropriate inner reference to simplify the electrode modification process. Recently, it has been reported that Cu_2O nanoparticles (NPs) show an oxidation peak at about − 0.1 V (vs. Ag/AgCl) in a pH 7.0 phosphate-buffer solution (PBS) and are used as the inner reference probe for the ratiometric detection of prostate specific antigen [20]. What is more, Cu_2O NPs are facile to prepare and display stable electrochemical activity.

MXene is a new family of two-dimension (2D) materials consisting of the transition metal nitrides/carbides/carbonitrides with the general formula of $M_{n+1}X_nT_x$ ($n = 1$, 2, or 3), where the M, X, and T stand for early transition metal, carbon, or/and nitrogen and the surface terminal groups (e.g., − O, − OH, − F), respectively [21]. Due to the excellent electrical conductivity, high specific surface area and hydrophilicity, MXene has aroused great attention of analysts [22]. $Ti_3C_2T_x$ is one of the representative materials of MXene, and is gradually applied to the field of electrochemical detection. For instance, alkalized $Ti_3C_2T_x$/MOF derived porous carbon composite was used as the modified material of electrode to monitor hydroquinone and catechol [23]. Park's group reported a $Ti_3C_2T_x$/MWCNT-modified flexible electrochemical sensor for the detection of Cu^{2+} and Zn^{2+} in human biofluids [24]. The previously reported work manifest that MXene can provide the in situ growth sites for Fe_3O_4 NPs, and its unique accordion-like structure facilitates the dispersion and immobilization of Fe_3O_4 NPs [25]. Inspired by this, Cu_2O NPs/$Ti_3C_2T_x$ composite can also be prepared in a similar method because $Ti_3C_2T_x$ shows good adsorption capacity toward heavy metallic ion (e.g., Pb^{2+}, Cu^{2+}) [24, 26].

Herein, ratiometric strategy was combined with MIP electrochemical sensor based on CNT/Cu_2O NPs/$Ti_3C_2T_x$ composite to detect DES. Cu_2O NPs was loaded on $Ti_3C_2T_x$ and used as an inner reference probe; CNT was introduced to increase the electrode surface and improve electrical conductivity. Finally, the MIP electrochemical sensor was prepared through the electropolymerization of 1H-pyrrole-3-carboxylicacid (py-3-COOH) in the presence of DES. The resulting ratiometric MIP electrochemical sensor (MIP/CNT/Cu_2O NPs/$Ti_3C_2T_x$/GCE) showed a satisfactory linear relationship and low detection limit for DES detection. Compared to the non-ratiometric MIP electrochemical sensor, the output signal fluctuation of the ratiometric MIP electrochemical sensor was much smaller. The sensor was successfully applied to determine DES in spiked real samples including lake water, milk, and pork.

Experimental

Preparation of CNT/Cu_2O NPs/$Ti_3C_2T_x$ composite

Accordion-like $Ti_3C_2T_x$ was prepared by etching the precursor Ti_3AlC_2 with HF according to previous reports with subtle modification [25].

Cu_2O NPs/$Ti_3C_2T_x$ composite was synthesized by in situ growth of Cu_2O NPs between the interlayers of accordion-like $Ti_3C_2T_x$. Briefly, 9 mg $CuCl_2{\cdot}H_2O$ was added into 50 mL of 0.2-mg mL^- $Ti_3C_2T_x$ dispersion and was ultrasonically treated for 30 min. Then, 0.4 mL of 0.5-M $N_2H_4{\cdot}H_2O$ solution was rapidly injected into the above dispersion and vigorously stirred for 15 min. The precipitation was obtained by centrifugation and washed with deionized water for three times, and dried overnight at 45 °C.

CNT/Cu_2O NPs/$Ti_3C_2T_x$ composite was obtained through the self-assembly method. CNT dispersion was firstly prepared by dispersing 1-mg CNT into 1 mL of 0.2-mg mL^{-1} CTAB solution under ultrasound for 2 h. Subsequently, 1 mL of 2 mg mL^{-1} Cu_2O NPs/$Ti_3C_2T_x$ composite dispersion was added and sonicated for 30 min. The mixture was centrifugated and rinsed with deionized water for five times, dried for 24 h at 45 °C. The procedure of preparing CNT/Cu_2O NPs/$Ti_3C_2T_x$ composite is illustrated in Scheme 1 A.

Fabrication of MIP/CNT/Cu_2O NPs/$Ti_3C_2T_x$/GCE

Bare GCEs were polished with 0.05-μm Al_2O_3 aqueous slurry and cleaned with deionized water under ultrasonic conditions. Then, 5 μL of CNT/Cu_2O NPs/$Ti_3C_2T_x$ composite (1 mg mL^{-1}) suspension was dropped on the cleaned GCE and dried at room temperature. The MIP film was

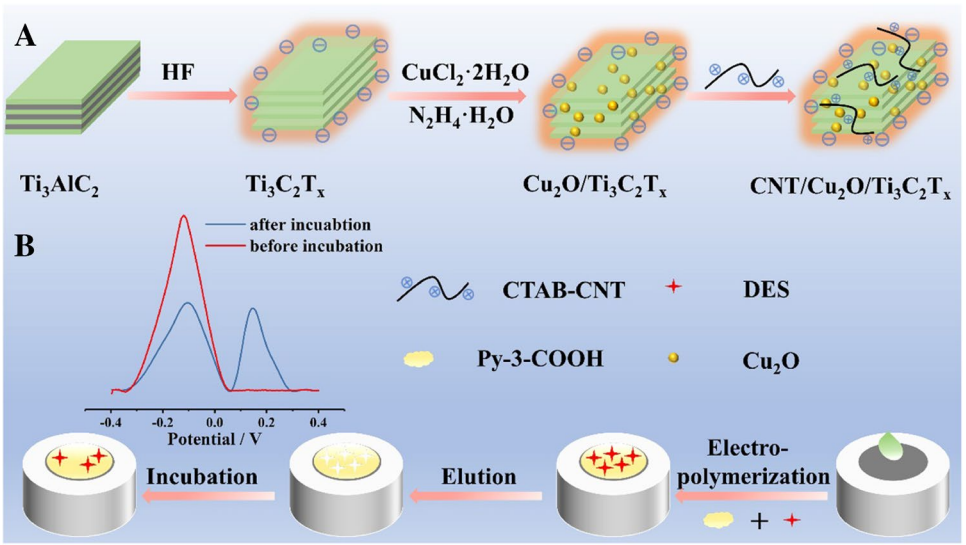

Scheme 1 Preparation processes of (**A**) CNT/Cu_2O NPs/$Ti_3C_2T_x$ and (**B**) MIP/CNT/Cu_2O NPs/$Ti_3C_2T_x$-modified electrode

synthesized by cyclic voltammetry (CV). The potential range was 0 ~ 0.8 V, the cycling number was 12 at a scan rate of 50 mV s^{-1}, and the solution was 0.1 − M PBS (pH 7.0) containing 2.4-mM py-3-COOH, 0.6-mM DES, and 0.1-M KCl. The templates were removed in 0.1-M NaOH/alcohol solution (V/V, 1:1) under stirring for 10 min. For comparison, non-imprinted polymer (NIP) was prepared by the same procedure but without DES. The preparation process of MIP/CNT/Cu_2O NPs/$Ti_3C_2T_x$/GCE is shown in Scheme 1 B.

Electrochemical measurements

The modified electrodes were characterized by CV and electrochemical impedance spectroscopy (EIS) in a mixed solution containing 5-mM $K_3[Fe(CN)_6]/K_4[Fe(CN)_6]$ and 0.1-M KCl. CV tests were performed in the potential range of − 0.2 V ~ 0.6 V at 100 mV/s. Parameters for EIS measurements were as follows: applied potential, 0.18 V; amplitude, 0.005 V; high frequency, 10^5 Hz; low frequency, 1 Hz. Differential pulse voltammetry (DPV) was applied to detect DES. The details were as follows: potential range, − 0.4 V ~ 0.4 V; amplitude, 50 mV; pulse width, 0.05 s; sample width, 0.0167 s; pulse period, 0.2 s.

Preparation of real samples

The water samples were collected from Wuhan East Lake and spiked with of DES standard solutions (1 mL) at different concentration levels, then filtered with $\Phi = 0.22$-μm nylon membrane. The milk and pork samples were bought from a local supermarket. Before measurement, the milk samples were mixed with 1 mL of DES standard solutions of different concentrations, then they were added into 20-mL alcohol and shaken for 15 min. After centrifuging at 10,000 rpm for 10 min, the supernatant was filtered with 0.22-μm nylon membrane and diluted to 50 mL with 0.1-M PBS (pH 7.5). As to pork samples, 4-g minced pork samples were spiked with 1 mL of DES standard solutions in a variety of concentrations; the mixture was transferred into 20-mL acetonitrile (contains 5% glacial acetic acid) and vigorously shaken for 15 min, followed by centrifugation at 10,000 rpm for 10 min. Then, the supernatant was extracted with 5 mL of n-hexane. Finally, the n-hexane layer was discarded, and the rest liquid was filtered with 0.22-μm nylon membrane and diluted to 50 mL with 0.1-M PBS (pH 7.5).

Results and discussion

Characterization of CNT/Cu_2O NPs/$Ti_3C_2T_x$ composite

The morphologies of composites were characterized by SEM and TEM. As could be seen in Fig. 1A, bulk Ti_3AlC_2 is closely aligned and layered. After treatment with HF solution, it became an accordion-like multi-layer structure, because the Al layers were selectively removed from the Ti_3AlC_2 phase using HF solution (Fig. 1B). As shown in Fig. 1C, Cu_2O NPs grow upon the surfaces and interlayers of $Ti_3C_2T_x$. This was related to the electrostatic and coordinated interaction between negative charged $Ti_3C_2T_x$ and Cu^{2+} [27]. In Fig. 1D, CNTs were coated on the surface of Cu_2O NPs/$Ti_3C_2T_x$ after the self-assemble treatment. As exhibited in Fig. 1E, the film forms on the surface of CNT/Cu_2O NPs/$Ti_3C_2T_x$ composite after the electropolymerization of py-3-COOH in the presence of DES. Figure 1F shows parts of Cu_2O NPs are agglomerated due to the high surface energy of Cu_2O NPs, and the interplanar space of $Ti_3C_2T_x$ is 1.02 nm (inserted HRTEM image in Fig. 1F).

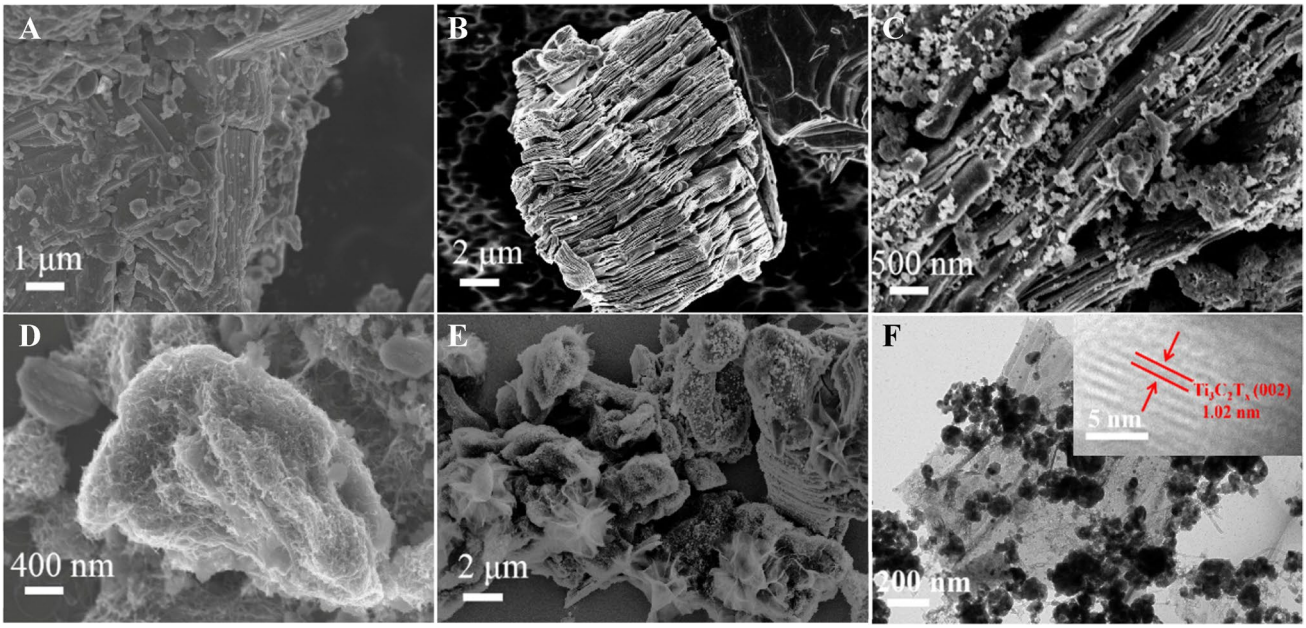

Fig. 1 SEM images of **A** Ti_3AlC_2, **B** $Ti_3C_2T_x$, **C** Cu_2O NPs/$Ti_3C_2T_x$, **D** CNT/Cu_2O NPs/$Ti_3C_2T_x$, and **E** MIP/CNT/Cu_2O NPs/$Ti_3C_2T_x$. TEM image of **F** CNT/Cu_2O NPs/$Ti_3C_2T_x$, and the insert image is the HRTEM of $Ti_3C_2T_x$

The preparation procedures of CNT/Cu_2O NPs/$Ti_3C_2T_x$ composite were also characterized by XRD. As shown in Fig. 2A, the characteristic diffraction peaks at 9.5° and 38.9° correspond to the (002) and (104) planes of Ti_3AlC_2, respectively. The curve b exhibited that the 38.9° peak disappeared while the 9.5° peak shifted to 8.9°, for the removal of Al phase from Ti_3AlC_2. The movement of (002) peak was in agreement with the HRTEM result; *d*-spacing of the as-prepared $Ti_3C_2T_x$ was wider than that of Ti_3AlC_2 ($d = 0.93$ nm) [28]. This manifested $Ti_3C_2T_x$ was prepared successfully. In curve c, diffraction peaks at 36.2 and 42.1° corresponded to the (111) and (200) lattice planes of Cu_2O NPs, respectively. The (002), (111), and (200) lattice planes appeared after the decoration of $Ti_3C_2T_x$ with Cu_2O NPs (curve d). In curve e, the diffraction intensity of $Ti_3C_2T_x$ and Cu_2O NPs decreased after the introduction of CNT. As shown in Fig. 2B, the zeta potential of the CNT/CTAB (1 mg mL^{-1} CNT dispersion containing 0.2 mg mL^{-1} CTAB) is measured to be + 40.1 mV. Therefore, electrostatic interaction must lead to the self-assembly of CNT and Cu_2O NPs/$Ti_3C_2T_x$. In addition, XPS results indicated the successful preparation of CNT/Cu_2O NPs/$Ti_3C_2T_x$ (Fig. S1).

Electrochemical characterization of the modified electrode

The EIS was used to characterize the interface change after every modification steps of the electrode. The diameter of the semicircle decreased after the Cu_2O NPs/GCE was successively modified with $Ti_3C_2T_x$ and CNT (Fig. 3A) due to the introduction of $Ti_3C_2T_x$ and CNT with good electrical conductivity. The electron transfer resistance (R_{et}) became

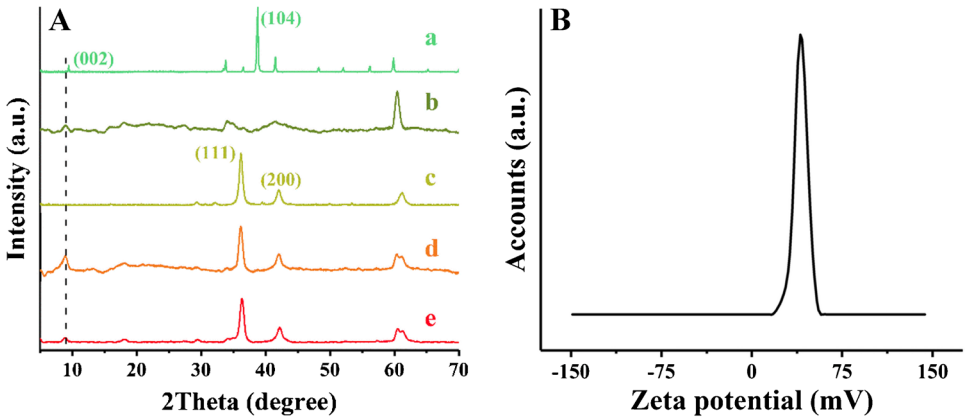

Fig. 2 **A** XRD patterns of (a) Ti_3AlC_2, (b) $Ti_3C_2T_x$, (c) Cu_2O NPs, (d) Cu_2O NPs/$Ti_3C_2T_x$, and (e) CNT/Cu_2O NPs/$Ti_3C_2T_x$. **B** Zeta potential of CNT/CTAB

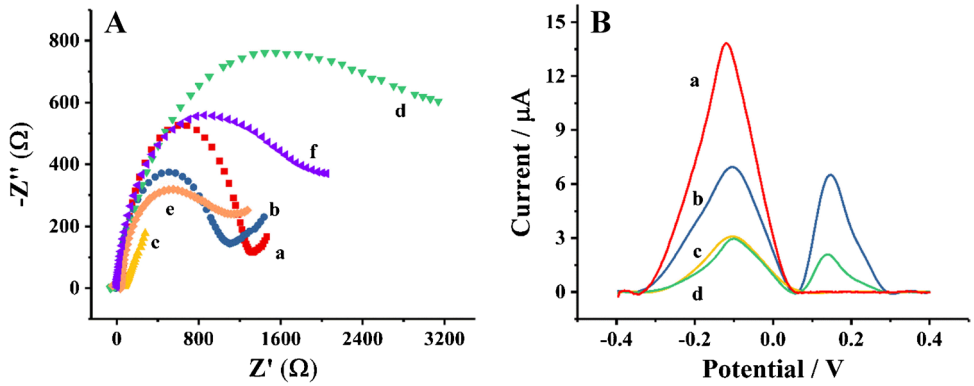

Fig. 3 **A** Nyquist plots of (a) Cu_2O/GCE, (b) $Cu_2O/Ti_3C_2T_x$/GCE, (c) CNT/$Cu_2O/Ti_3C_2T_x$/GCE, (d) MIP/CNT/$Cu_2O/Ti_3C_2T_x$/GCE before the removal of template, (e) MIP/CNT/$Cu_2O/Ti_3C_2T_x$/GCE after the removal of template, (f) MIP/CNT/$Cu_2O/Ti_3C_2T_x$/GCE after incubation in 50-μM DES. The tests were completed in 5-mM $[Fe(CN)_6]^{3-/4-}$ containing 0.1-M KCl. **B** DPV curves of MIP/CNT/Cu_2O NPs/$Ti_3C_2T_x$/GCE (a) before and (b) after incubation, NIP/CNT/Cu_2O NPs/$Ti_3C_2T_x$/GCE in PBS (c) before and (d) after incubation. Incubation solution, PBS (pH 7.5, 0.1 M) containing 50-μM DES

large drastically after the polymerization of py-3-COOH in the presence of DES indicating the MIP film had poor conductivity. The R_{et} decreased after removing the DES from the MIP film as the binding cavities facilitated the probe to pass through the MIP films. However, when the MIP/CNT/Cu_2O NPs/$Ti_3C_2T_x$/GCE was incubated in PBS containing DES, R_{et} increased for the blocking of binding sites. CV measurements were also conducted, and the results agreed with the EIS data (Fig. S2).

To illustrate the specific adsorption of MIP, DPV curves of MIP and NIP-modified CNT/Cu_2O NPs/$Ti_3C_2T_x$/GCE before and after incubation in 50-μM DES were presented (Fig. 3B). The peaks at − 0.11 V and 0.14 V were assigned to Cu_2O NPs and DES, respectively. The I_{DES} increased while the ICu_2O decreased after the rebinding of DES. The reason was that the cavities of MIP film were occupied by DES which led to the partial block of electron transfer channel toward Cu_2O NPs, thus the signal of Cu_2O NPs decreased. However, the ICu_2O for NIP film almost remained unchanged after the incubation of DES, indicating there were no cavities formed in the NIP film (curve c and curve d).

Optimization of the experiment conditions

To improve the analytical capacity of the as-prepared MIP electrochemical sensor, optimization of experiment conditions including the molar ratio of monomer to template, polymerization cycles, pH, and incubation time were performed.

Polymer structure and rebinding capacity of MIP sensors were influenced by the monomer/template ratio. As shown in Fig. S3A, the value of I_{DES}/ICu_2O increases with the increase of py-3-COOH/DES ratio, for the formed MIP film becomes denser and has more imprinted cavities. However, py-3-COOH/DES ratio higher than 4:1 would also lead to the decrease of I_{DES}/ICu_2O, because the recognition sites were blocked by excess py-3-COOH. Therefore, the optimum ratio of py-3-COOH/DES was 4:1.

The thickness of MIP film greatly affected the number of recognition sites, which could be adjusted by changing the polymerization cycles. Thinner MIP film could not provide enough recognition sites, while the thicker MIP film was unfavorable for the removal of DES. The MIP film with the optimum thickness was obtained through 12 polymerization cycles (Fig. S3B).

The influence of pH on the sensing response was investigated from 6.0 to 8.5 (Fig. S3C). The I_{DES}/ICu_2O value increased as the pH increased from 6 to 7.5, the electro-oxidization reaction of DES was boosted at low acidity for the protons of DES were released in this process. At pH 7.5, the I_{DES}/ICu_2O value was the highest. When pH further increased, the I_{DES}/ICu_2O value decreased when the pH further increased, which might result from the dissociation of DES in alkaline solution [29].

Linear relationships between the oxidation potential of DES and Cu_2O NPs and pH are shown in Fig. S3D;, their slopes were calculated to be − 52.3 mV and − 54.1 mV, respectively. It manifested that the number of electrons and protons involved in the redox of DES and Cu_2O NPs was the same.

The optimum incubation time is 5 min according to Fig. S2E.

Stability of ratiometric electrochemical sensor

Robustness of inner reference signal is essential to the ratiometric electrochemical sensor. Here, DPV curves of CNT/

Cu_2O NPs/$Ti_3C_2T_x$/GCE in PBS (pH 7.5) for ten consecutive tests were basically the same; the oxidation peak of Cu_2O remained constant (Fig. 4A). The signal stability of Cu_2O NPs/GCE and Cu_2O NPs/$Ti_3C_2T_x$/GCE was also explored. The results illustrated that the incorporation of $Ti_3C_2T_x$ could effectively stabilize the response of the Cu_2O NPs (Fig. S4). To illustrate the stability of the output signal of the as-prepared ratiometric electrochemical sensor, the DPV curves of three different MIP/CNT/Cu_2O NPs/$Ti_3C_2T_x$/GCE were recorded after incubation (Fig. 4B). The ratio values of I_{DES}/ICu_2O almost remained unchanged while the values of I_{DES} fluctuate greatly. To further verify the advantage of ratiometric strategy, the I_{DES} and I_{DES}/ICu_2O data were collected and compared after ten paralleled tests were conducted with MIP/CNT/Cu_2O NPs/$Ti_3C_2T_x$/GCE (Fig. 4C). The RSD of non-ratiometric sensor was 8.5% while that of the ratiometric sensor was 3.3%. This showed that the introduction of ratiometric strategy reduced the error caused by personal manipulation and changes in the surface of electrode, which helped to obtain more reliable data.

Analytical performance of ratiometric electrochemical sensor

The performance of MIP/CNT/Cu_2O NPs/$Ti_3C_2T_x$/GCE was evaluated through DPV technique under optimized conditions. The MIP/CNT/Cu_2O NPs/$Ti_3C_2T_x$/GCE was incubated in 0.1-M PBS (pH 7.5) containing different concentrations of DES. As depicted in Fig. 5A, the peak current of Cu_2O NPs decreases, while the peak current of DES increases with the increase of DES concentration. The sensor showed a good linear relationship between I_{DES}/ICu_2O and C_{DES} in the range from 0.01 to 70 μM (Fig. 5B). The linear equation was $I_{DES}/ICu_2O = 0.0183 \times C_{DES} + 0.00502$ ($R^2 = 0.9928$), and the limit of detection ($S/N = 3$) was calculated to be 6 nM.

Selectivity, repeatability and lifetime

To investigate the selectivity of MIP/CNT/Cu_2O NPs/$Ti_3C_2T_x$/GCE, the analogs of DES (i.e., E1, E2, BPA, BPS, and TBBPA) were chosen as the interference substances. The concentrations of DES and interference substances were 30 μM and 300 μM, respectively. As shown in Fig. 6A, the deviation of the I_{DES}/ICu_2O values are lower than 5.8%, indicating that the MIP/CNT/Cu_2O NPs/$Ti_3C_2T_x$/GCE possesses satisfactory selectivity toward DES. The reason was that DES could be selectively adsorbed by the MIP film through hydrogen bond and the spatial structure matching between DES and imprinted cavities (Fig. 6B).

The repeatability was evaluated by five consecutive measurements of 50-μM DES using one electrode. The RSD value of I_{DES}/ICu_2O was 4.3%, indicating the satisfactory repeatability of the as-prepared electrode.

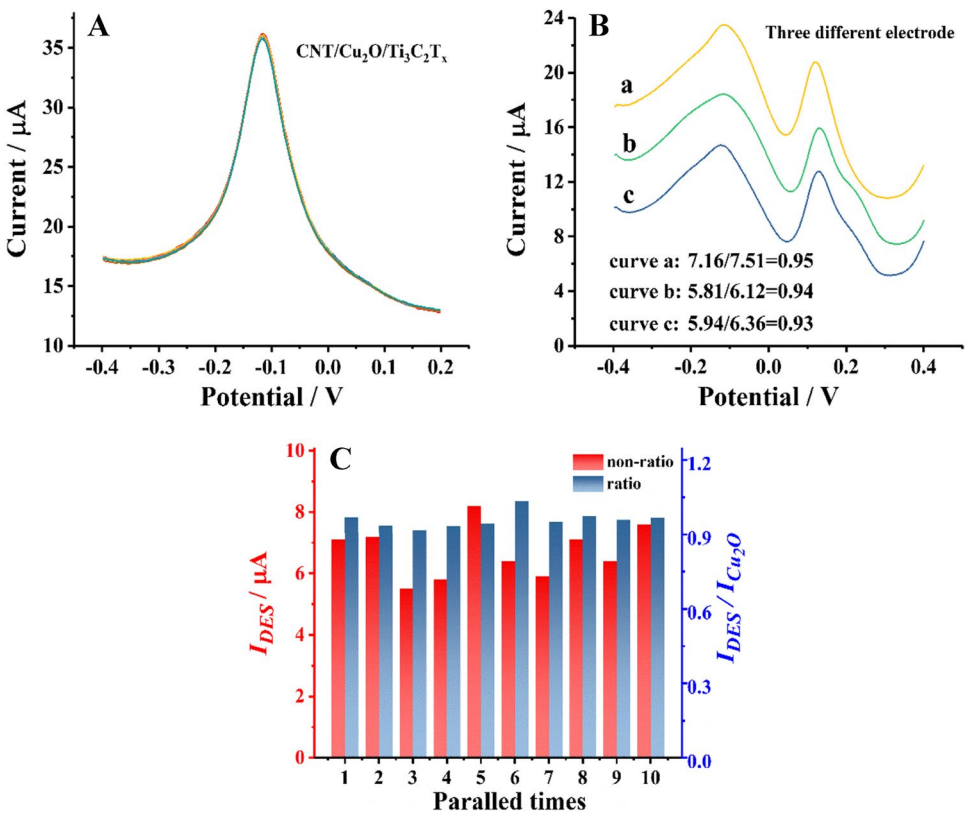

Fig. 4 **A** Consecutive tests of CNT/Cu_2O NPs/$Ti_3C_2T_x$/GCE in PBS (pH 7.5). **B** DPV curves of three different MIP/CNT/Cu_2O NPs/$Ti_3C_2T_x$/GCE after incubation with 50-μM DES. (C) I_{DES} and I_{DES}/ICu_2O data collected by ten different MIP/CNT/Cu_2O NPs/$Ti_3C_2T_x$/GCE after incubation with 50 μM DES

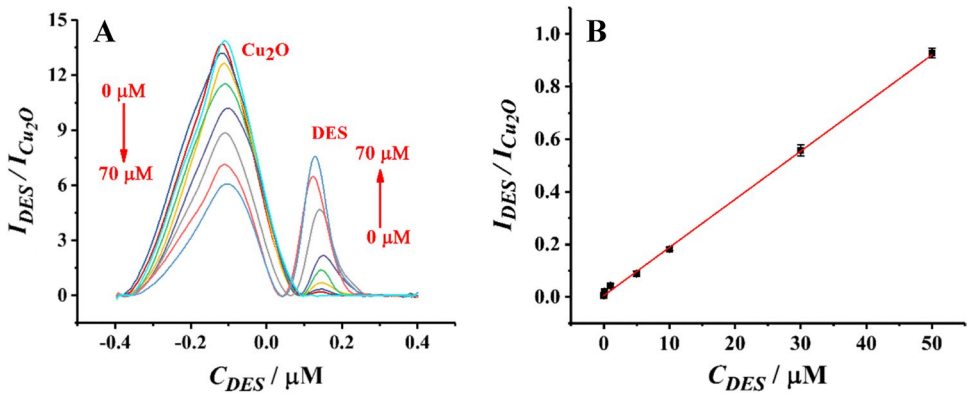

Fig. 5 **A** DPV responses and **B** calibration curves of the MIP/CNT/Cu_2O NPs/$Ti_3C_2T_x$ electrodes after incubation in 0.1-M PBS (pH 7.5) containing different concentrations of DES ($n = 3$)

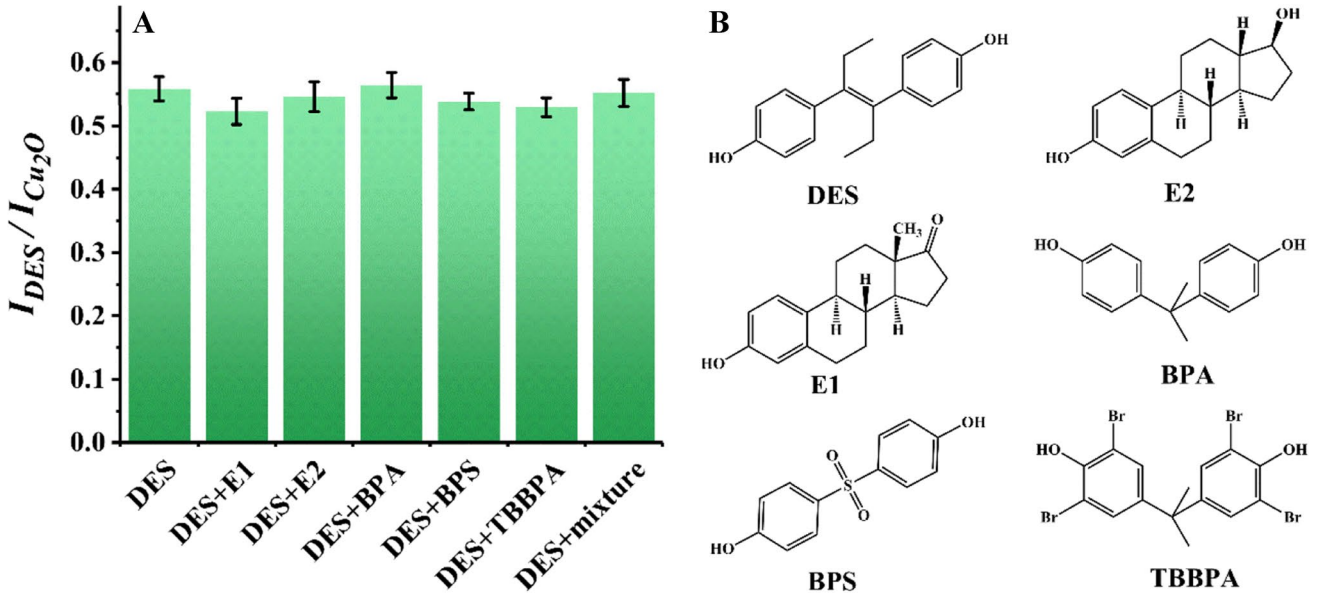

Fig. 6 **A** Responses of MIP/CNT/Cu_2O NPs/$Ti_3C_2T_x$/GCE after incubation in 30-μM DES alone or in 30-μM DES plus 300-μM analogs ($n = 3$). (**B**) Structural formula of DES and its analogs

To research the lifetime, the as-prepared electrodes which had been stored at 4 °C for 3 weeks were applied to detect 50-μM DES in PBS (pH = 7.5). The value of I_{DES}/ICu_2O is only 5.3% lower than that of the initial detection. The results showed the as-prepared electrodes possessed good stability.

As shown in Table 1, although the immunosensors exhibit lower limit of detection, they are generally disposable, whereas the as-prepared MIP sensor in this work can be reused. Furthermore, the immunosensors are expensive and take a long time for analysis. Compared with the electrochemical sensors without a specific recognition device (Table 1), which typically distinguish interferences by potential, as described in the "Introduction", the as-prepared MIP sensor in this work not only shows a lower limit of detection but also possesses good selectivity.

Analysis of real samples

To evaluate its practical analytic performance, the as-prepared sensor was applied to determine DES in real samples, including lake water, milk, and pork. As shown in Table 2, there no DES were found in the pretreated real samples using the as-prepared sensor and HPLC. After that, the real samples were spiked at three concentration levels (0.05 μM, 0.1 μM, and 1 μM). The recoveries of the spiked samples were 88–112%, and the RSD ranged from 3.6 to 5.5%. In order to verify the results obtained by the as-prepared sensor, HPLC measurements of the spiked real sample solutions were performed; it manifested that the concentrations detected by the as-prepared sensor were close to HPLC detection results. Therefore, the MIP/CNT/Cu_2O NPs/$Ti_3C_2T_x$/GCE exhibited good practicality for DES detection in real samples.

Table 1 Comparison of proposed method for DES with others

Detection methods	Linear range (mol/L)	Detection limit (mol/L)	Refs
Graphene/GNPs[a]/GCE	1.2×10^{-8}–1.2×10^{-5}	9.8×10^{-9}	[30]
ERGO[b]/GCE	9.0×10^{-8}–1.0×10^{-5}	8×10^{-8}	[31]
WMMIPs[c]/MWCNTs@CS[d]/CTABr/MGCE[e]	1.5×10^{-9}–1.5×10^{-4}	2.5×10^{-10}	[29]
Ab/MSN[f]/GNPs/MWCNTs and HRP[g]-Ab/GNPs/PB[h]/MWCNTs biocon-jugates	5.0×10^{-9}–1.7×10^{-5}	4.5×10^{-10}	[32]
Ab/Ag NPs/$Cu_3(BTC^i)_2$ and α-Fe_2O_3/BSA-DES immunosensor	1.8×10^{-11}–1.8×10^{-9}	6.2×10^{-11}	[33]
MIP/CNT/Cu_2O NPs/$Ti_3C_2T_x$/GCE	1.0×10^{-8}–7.0×10^{-5}	6.0×10^{-9}	This work

[a]Gold nanoparticles

[b]Electrochemical reduced graphene oxide

[c]Water-compatible magnetic MIPs

[d]Chitosan

[e]Magnetic glass carbon electrode

[f]Mesoporous silica nanoparticles

[g]Horseradish peroxidase

[h]Prussian blue

[i]1,3,5-Benzenetricarboxylate

Table 2 Determination of DES in real samples with the as-prepared sensor

Samples	DES added (μM)	HPLC	As-prepared sensor		
		Found (μM)	Found (μM)	Recovery (%, $n=3$)	RSD (%, $n=3$)
Lake water	0	Not found	Not found	-	-
	0.05	0.052	0.053	106	4.9
	0.1	0.094	0.088	88	4.3
	1.00	0.97	0.95	95	3.8
Milk	0	Not found	Not found	-	-
	0.05	0.053	0.056	112	5.1
	0.1	0.096	0.093	93	3.6
	1.00	1.03	1.07	107	4.4
Pork	0	Not found	Not found	-	-
	0.05	0.054	0.045	90	5.5
	0.1	0.097	0.091	91	5.3
	1.00	1.01	0.95	95	4.7

Conclusions

In this work, we developed a ratiometric MIP electrochemical sensor for diethylstilbestrol detection based on the CNT/Cu_2O NPs/$Ti_3C_2T_x$ composite using the Cu_2O NPs as the inner reference. The accordion-like structure of $Ti_3C_2T_x$ was beneficial to the in situ growth and fixation of Cu_2O NPs, resulting in the increase of signal stability of Cu_2O NPs. Furthermore, choosing Cu_2O NPs as the inner reference could reduce the electrode modification steps. The as-prepared sensor showed good detection performance toward DES in real samples, which provided a new thought for DES reliable detection. Although the ratiometric strategy can effectively reduce the fluctuation of the output signal, some limitations in electrochemical sensor are existed. For example, the fouling of the electrode in the complex determination environment is unavoidable, resulting in the decrease of the electrochemical signal. Therefore, improving the anti-fouling property of the modified electrode is necessary.

Supplementary Information The online version contains supplementary material available at https://doi.org/10.1007/s00604-022-05249-x.

Funding This work was supported by the financial support of the National Natural Science Foundation of China (grant numbers 21775112).

Declarations

Conflict of interest The authors declare no competing interests.

References

1. Liu M, Li M, Qiu B, Chen X, Chen G (2010) Synthesis and applications of diethylstilbestrol-based molecularly imprinted polymer-coated hollow fiber tube. Anal Chim Acta 663:33–38
2. Zhao WR, Kang TF, Lu LP, Cheng SY (2018) Magnetic surface molecularly imprinted poly(3-aminophenylboronic acid) for selective capture and determination of diethylstilbestrol. RSC Adv 8:13129–13141
3. Qiao L, Gan N, Hu F, Wang D, Lan H, Li T, Wang H (2014) Magnetic nanospheres with a molecularly imprinted shell for the preconcentration of diethylstilbestrol. Microchim Acta 181:1341–1351
4. Judson R, Richard A, Dix DJ, Houck K, Martin M, Kavlock R, Dellarco V, Henry T, Holderman T, Sayre P, Tan S, Carpenter T, Smith E (2009) The toxicity data landscape for environmental chemicals. Environ Health Perspect 117:685–695
5. Zhang J, Zang L, Wang T, Wang X, Jia M, Zhang D, Zhang H (2020) A solid-phase extraction method for estrogenic disrupting compounds based on the estrogen response element. Food Chem 333:127529
6. Qiao Q, Shi N, Feng X, Lu J, Han Y, Xue C (2016) Diethylstilbestrol in fish tissue determined through subcritical fluid extraction and with GC-MS. J Ocean Univ China 15:489–494
7. Liu SF, Xie ZH, Wu XP, Lin XC, Guo LQ, Chen GN (2005) Separation of structurally related estrogens using isocratic elution pressurized capillary electrochromatography. J Chromatogr A 1092:258–262
8. Yang X, Wang Y, Song C, Hu X, Wang F, Zeng X (2020) Hapten synthesis and the development of an ultrasensitive indirect competitive eLISA for the determination of diethylstilbestrol in food samples. Sci Rep 10:3270
9. Mi J, Dong X, Zhang X, Li C, Wang J, Mujtaba MG, Zhang S, Wen K, Yu X, Wang Z (2019) Novel hapten design, antibody recognition mechanism study, and a highly sensitive immunoassay for diethylstilbestrol in shrimp. Anal Bioanal Chem 411:5255–5265
10. Chen X, Shi Z, Hu Y, Xiao X, Li G (2018) A novel electrochemical sensor based on Fe_3O_4-doped nanoporous carbon for simultaneous determination of diethylstilbestrol and 17 beta-estradiol in toner. Talanta 188:81–90
11. Wu J, Zhao X, Zou Y, Wu X, Bai W, Zeng X (2021) Electrochemical determination of diethylstilbestrol in livestock and poultry meats by L-cysteine/gold nanoparticles modified electrode. Microchem J 164
12. Li C, Zhang Y, Zeng T, Chen X, Wang W, Wan Q, Yang N (2019) Graphene nanoplatelet supported CeO_2 nanocomposites towards electrocatalytic oxidation of multiple phenolic pollutants. Anal Chim Acta 1088:45–53
13. Ji L, Wang Y, Wu K, Zhang W (2016) Simultaneous determination of environmental estrogens: diethylstilbestrol and estradiol using Cu-BTC frameworks-sensitized electrode. Talanta 159:215–221
14. Crapnell RD, Hudson A, Foster CW, Eersels K, Van Grinsven B, Cleij TJ, Banks CE, Peeters M (2019) Recent advances in electrosynthesized molecularly imprinted polymer sensing platforms for bioanalyte detection. Sensors 19:1204
15. Jin H, Gui R, Yu J, Lv W, Wang Z (2017) Fabrication strategies, sensing modes and analytical applications of ratiometric electrochemical biosensors. Biosens Bioelectron 91:523–537
16. Yang J, Hu Y, Li Y (2019) Molecularly imprinted polymer-decorated signal on-off ratiometric electrochemical sensor for selective and robust dopamine detection. Biosens Bioelectron 135:224–230
17. Wang XY, Feng YG, Wang AJ, Mei LP, Yuan PX, Luo X, Feng JJ (2021) A facile ratiometric electrochemical strategy for ultrasensitive monitoring HER2 using polydopamine-grafted-ferrocene/reduced graphene oxide, Au@Ag nanoshuttles and hollow Ni@PtNi yolk-shell nanocages. Sensor Actuat B-Chem 331:129460
18. Zhang W, Liu C, Han K, Wei X, Xu Y, Zou X, Zhang H, Chen Z (2020) A signal on-off ratiometric electrochemical sensor coupled with a molecular imprinted polymer for selective and stable determination of imidacloprid. Biosens Bioelectron 154:112091
19. Zhang R, Liu J, Li Y (2019) MXene with great adsorption ability toward organic dye: an excellent material for constructing a ratiometric electrochemical sensing platform. ACS Sens 4:2058–2064
20. Zhao Y, Liu H, Shi L, Zheng W, Jing X (2020) Electroactive Cu_2O nanoparticles and Ag nanoparticles driven ratiometric electrochemical aptasensor for prostate specific antigen detection. Sensor Actuat B-Chem 315:128155
21. Alhabeb M, Maleski K, Anasori B, Lelyukh P, Clark L, Sin S, Gogotsi Y (2017) Guidelines for synthesis and processing of two-dimensional titanium carbide ($Ti_3C_2T_X$ MXene). Chem Mater 29:7633–7644
22. Sajid M (2021) MXenes: are they emerging materials for analytical chemistry applications? - A review. Anal Chim Acta 1143:267–280
23. Huang R, Liao D, Chen S, Yu J, Jiang X (2020) A strategy for effective electrochemical detection of hydroquinone and catechol: decoration of alkalization-intercalated Ti_3C_2 with MOF-derived N-doped porous carbon. Sensor Actuat B-Chem 320:128386
24. Hui X, Sharifuzzaman M, Sharma S, Xuan X, Zhang S, Ko SG, Yoon SH, Park JY (2020) High-performance flexible electrochemical heavy metal sensor based on layer-by-layer assembly of $Ti_3C_2T_x$/MWNTs nanocomposites for noninvasive detection of copper and zinc ions in human biofluids. ACS Appl Mater Inter 12:48928–48937
25. Zhang Q, Teng J, Zou G, Peng Q, Du Q, Jiao T, Xiang J (2016) Efficient phosphate sequestration for water purification by unique sandwich-like MXene/magnetic iron oxide nanocomposites. Nanoscale 8:7085–7093
26. Peng Q, Guo J, Zhang Q, Xiang J, Liu B, Zhou A, Liu R, Tian Y (2014) Unique lead adsorption behavior of activated hydroxyl group in two-dimensional titanium carbide. J Am Chem Soc 136:4113–4116
27. Xie H, Li P, Shao J, Huang H, Chen Y, Jiang Z, Chu PK, Yu XF (2019) Self-assembly of $Ti_3C_2T_x$ MXene and gold nanorods as an efficient surface-enhanced Raman scattering platform for reliable and high-sensitivity determination of organic pollutants. ACS Sens 4:2303–2310
28. Husmann S, Budak SH, Liang K, Aslan M, Kruth A, Quade A, Naguib M, Presser V (2020) Ionic liquid-based synthesis of MXene. Chem Commun 56:11082–11085
29. Zhao W-R, Kang T-F, Lu L-P, Cheng S-Y (2018) Electrochemical magnetic imprinted sensor based on MWCNTs@CS/CTABr surfactant composites for sensitive sensing of diethylstilbestrol. J Electroanal Chem 818:181–190
30. Ma X, Chen M (2015) Electrochemical sensor based on graphene doped gold nanoparticles modified electrode for detection of diethylstilboestrol. Sensor Actuat B-Chem 215:445–450
31. Zhu X, Lu L, Duan X, Zhang K, Xu J, Hu D, Sun H, Dong L, Gao Y, Wu Y (2014) Efficient synthesis of graphene-multiwalled carbon nanotubes nanocomposite and its application in electrochemical sensing of diethylstilbestrol. J Electroanal Chem 731:84–92

32. Liu S, Lin Q, Zhang X, He X, Xing X, Lian W, Li J, Cui M, Huang J (2012) Electrochemical immunosensor based on mesoporous nanocomposites and HRP-functionalized nanoparticles bioconjugates for sensitivity enhanced detection of diethylstilbestrol. Sensor Actuat B-Chem 166:562–568
33. Li X, Miao J, Li Y, Liu L, Dong X, Zhao G, Fang J, Wei Q, Cao W (2019) Copper-based metal-organic frameworks loaded with silver nanoparticles as electrochemical immunosensors for diethylstilbestrol. ACS Appl Nano Mater 2:8043–8050